DNA Structures

DOI: 10.1002/ange.201101759

Kinetic and Thermodynamic Control of G-Quadruplex Folding**

*Yong Xue, Jia-quan Liu, Ke-wei Zheng, Zhong-yuan Kan, Yu-hua Hao, and Zheng Tan**

G-quadruplexes, which are unique four-stranded structures formed by guanine-rich (G-rich) nucleic acids, are enriched in essential regions in genomes and are implicated in the regulation of gene expression at both transcription and translation levels. These structures are becoming promising therapeutic targets against cancer and other diseases.[1] G-quadruplexes are highly polymorphic in their folding topology,[2] which is sensitive to the sequence composition, the loop size,[3] and surrounding environmental factors, such as species of cations,[4] and the presence of chemical ligands[5] and crowding agents.[6] The control of G-quadruplex folding and its physiological relevance is not only important for understanding the in vivo function of a G-quadruplex, but also for developing effective drugs.[7]

To date, the vast majority of studies have focused on DNA structures in the thermodynamic equilibrium state. However, many biological processes that are essential in gene expression, such as chromatin remodeling and transcriptional control, are mostly regulated by kinetic control. Specifically, nucleic acids inside cells are bound to proteins or other biomolecules, such as complementary strands, and are only liberated during specific physiological processes, such as DNA replication and transcription. Potential G-quadruplex formation during these processes might be dominated by kinetic rather than thermodynamic control. This issue represents a potentially important, but hitherto neglected topic in the field.

We have studied the kinetic versus thermodynamic control of G-quadruplex folding by using human telomere DNA as a model system. By employing circular dichroism, fluorescence spectroscopy, gel electrophoresis, and photocleavage footprinting, we show that when liberated from the DNA duplex upon duplex disruption or helicase unwinding, human telomere DNA initially forms a distinct structure from the one it forms at the equilibrium state in a K^+/PEG solution. This result demonstrates that the conformation initially adopted by a G-quadruplex in physiological events may not be the one that it adopts in the equilibrium state, and that the competition between kinetic and thermodynamic control is an important factor in determining the biological and pharmaceutical relevance of a G-quadruplex.

G-quadruplex formation during duplex disruption was first studied in a hairpin duplex DNA, which was prepared in a 150 mM K^+ solution (see Figure S1 in the Supporting Information) and then rapidly mixed into an equimolar K^+ solution containing 40% PEG 200. PEG 200 has been shown to affect the conformation of G-quadruplexes.[6a,b,8] In particular, PEG 200 dramatically destabilizes DNA duplexes and stabilizes G-quadruplexes.[8a–c,9] As a result, the duplex was disrupted and the G-rich region folded into a G-quadruplex when PEG was added.[9b]

Figure 1 shows the CD spectra that were used to monitor the structural changes. Initially, the original hairpin in the K^+ solution displayed a negative peak at 240 nm and a positive

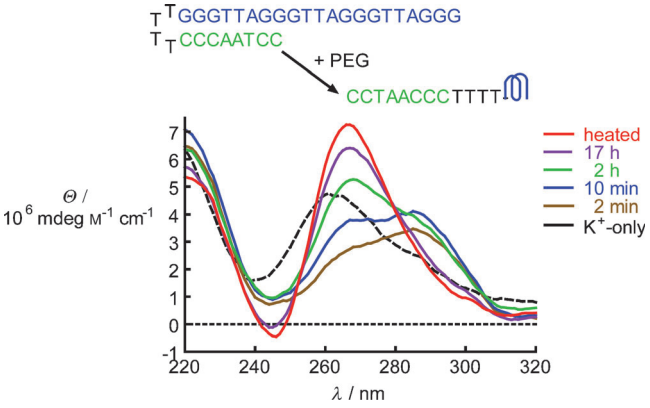

Figure 1. G-quadruplex formation and structural transition in a DNA duplex carrying the core telomere sequence $G_3(T_2AG_3)_3$ at the 3′ end monitored by CD spectroscopy. The DNA hairpin originally formed in a 150 mM K^+ buffer converted into a G-quadruplex when the sample was mixed with an equal volume of the same buffer containing 80% (w/v) PEG 200. CD spectra were collected at the indicated time after mixing at 37°C. PEG = poly(ethylene glycol).

peak at 260 nm, which are characteristic of a DNA duplex.[10] Shortly after PEG was added, a positive peak near 285 nm emerged. The parallel/antiparallel hybrid human telomere G-quadruplex features a positive peak near 290 nm,[5a,11] and the parallel form displays a negative peak near 240 nm followed by a positive peak near 265 nm[6a] as for many other telomere sequences.[6b,c,10b,12]

[*] Y. Xue,[+] Y.-h. Hao, Prof. Dr. Z. Tan
State Key Laboratory of Biomembrane and Membrane Biotechnology, Institute of Zoology
Chinese Academy of Sciences, Beijing 100101 (China)
E-mail: z.tan@ioz.ac.cn
tanclswu@public.wh.hb.cn
Homepage: http://www.biomembrane.ioz.ac.cn/Entanz.asp
J.-q. Liu,[+] K.-w. Zheng, Z.-y. Kan
Laboratory of Biochemistry and Biophysics
College of Life Sciences
Wuhan University, Wuhan 430072 (China)
[+] These authors contributed equally to this work.

[**] This work was supported by grants from the MSTC (2010CB945300) and the NSFC (90813031, 30970617, 21072189, and 20921062). We are grateful to Dr. Ian Hickson at the University of Oxford (UK) for providing the pJK1 plasmid.

Supporting information for this article (including experimental details) is available on the WWW under http://dx.doi.org/10.1002/anie.201101759.

The appearance of the new peak near 285 nm suggests that the G-quadruplex might initially assume a parallel/antiparallel structure upon hairpin duplex disruption and then gradually convert to a parallel structure, as judged from the disappearance of the peak near 285 nm and the emergence of a positive peak near 265 nm. The spectra gradually approached that of the parallel G-quadruplex at the equilibrium state, which was prepared by heat denaturation/renaturation and featured a positive peak at 265 nm and a negative peak at 245 nm.[6a]

At the equilibrium state, the human telomere G-quadruplex adopts a parallel/antiparallel hybrid structure in K^+ solution,[11b,c,13] but a parallel propeller-like structure in K^+ solution containing 40% PEG 200,[6a] as it does in K^+-containing crystals.[14] Our CD results suggest that the DNA, when given a chance to fold in the K^+/PEG solution, might initially adopt a structure that is not the one it adopts at the equilibrium state in the same solution.

Further analyses were carried out to verify the observation by using a format that mimics the separation of the DNA duplex in vivo, because CD spectroscopy is not a definitive indicator of folding orientation.[15] Here, the G-rich telomere strand $G_3(T_2AG_3)_3$ was annealed to a longer complementary C-rich strand in such a way that the 3′ region of the C-rich strand protruded out in a single-stranded form (Figure 2).

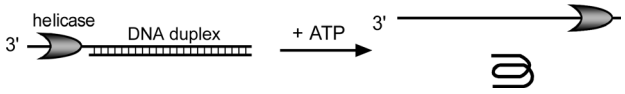

Figure 2. G-quadruplex formation of $G_3(T_2AG_3)_3$ released from the DNA duplex by Bloom syndrome (BLM) helicase upon addition of adenosine triphosphate (ATP).

Because of the intermolecular nature, the duplex was prepared at a 5 μM strand concentration in a K^+ solution to ensure duplex formation (see Figure S2 in the Supporting Information), and then diluted 100 times into a K^+ or a K^+/PEG solution containing BLM helicase. After a brief incubation for the helicase to load onto the overhang, the $G_3(T_2AG_3)_3$ was released from the C-rich strand by the helicase, catalyzed by the addition of ATP (see Figure 2, and Figure S3 in the Supporting Information).[16]

The released strand $G_3(T_2AG_3)_3$ formed a G-quadruplex, as verified by fluorescence resonance energy transfer (FRET) between the two fluorophores labeled at the two ends of the $G_3(T_2AG_3)_3$ (see Figure S3 in the Supporting Information). Because of the requirement of a high DNA concentration (μM level) and, as a result, a high concentration of helicase, we were unable to monitor the G-quadruplex formation by CD spectroscopy. Therefore, the formation of the G-quadruplex was next examined using $G_3(T_2AG_3)_3$ substituted with 2-aminopurine (Ap) at different adenine residues (Figure 3). Ap is a fluorescent adenine isomer whose fluorescence is sensitive to local conformational changes in DNA, and it has been used to probe the structure of human telomere G-quadruplexes.[6a,17] In particular, Ap was used to distinguish parallel telomere G-quadruplexes from antiparallel/parallel

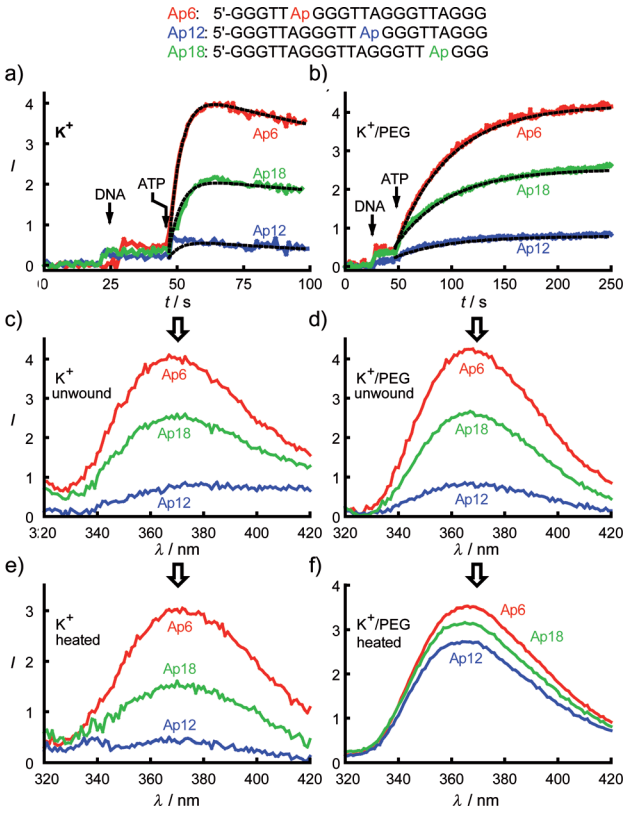

Figure 3. G-quadruplex formation of $G_3(T_2AG_3)_3$ released from the DNA duplex by BLM helicase monitored by the fluorescence of the Ap substituent at different loop positions. Unwinding in a 150 mM K^+ solution in the absence (a) or in the presence (b) of 40% (w/v) PEG 200 was initiated by the addition of ATP, and the fluorescence was recorded over time at 37°C. After unwinding, the emission spectrum of each sample was scanned immediately (c,d) or after a heat denaturation/renaturation treatment (e,f). A 20-fold excess of unlabeled $G_3(T_2AG_3)_3$ was added before the heat treatment to prevent the Ap DNA from re-annealing into a duplex. Dotted black lines in (a) and (b) are theoretical lines obtained by fitting the curves to a sequential two-step first-order and a simple first-order reaction, respectively.

ones in K^+ solutions.[6a] The relative fluorescence intensities of the Ap dyes in the three loops of the parallel/antiparallel K^+ G-quadruplex are in the order Ap6 > Ap18 > Ap12, with large differences.[6a,17] The emission from Ap6 is about seven times higher than that from Ap12.[6a,17a] For the parallel K^+/PEG G-quadruplex, the fluorescence of each of the three Ap dyes is very similar because of the structural symmetry of the three external TTA loops. In this case, the fluorescence ratio of Ap6 to Ap12 is slightly larger than one.[6a]

Figure 3a–d shows G-quadruplex formation as the $G_3(T_2AG_3)_3$ was released from the duplex. The fluorescence of Ap is quenched in the DNA duplex,[18] thus the formation of the G-quadruplex led to an increase in fluorescence (Figure 3a,b). The ratio and order of fluorescence intensities of the three Ap dyes clearly show that the same parallel/antiparallel hybrid G-quadruplex was formed in both the absence (Figure 3a,c) and the presence (Figure 3b,d) of PEG, and is consistent with the structure adopted in the K^+ solution (Figure 3e) instead of the one adopted in the K^+/

PEG solution (Figure 3 f) at the equilibrium state by this DNA after a heat denaturation/renaturation treatment.[6a] Thus, these results support that the $G_3(T_2AG_3)_3$ initially formed a parallel/antiparallel hybrid G-quadruplex in the K^+/PEG solution rather than the parallel one it formed in the equilibrium state.

The G-quadruplex structure that was adopted by the $G_3(T_2AG_3)_3$ and released by duplex unwinding was further verified by gel electrophoresis (Figure 4). The parallel form of

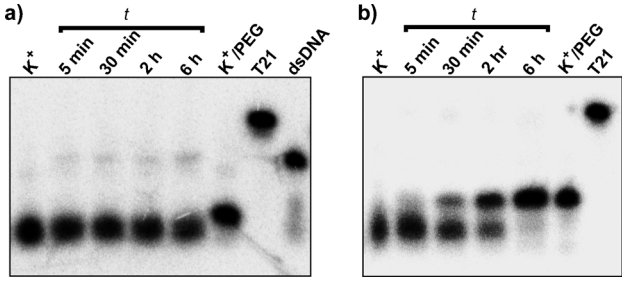

Figure 4. G-quadruplex formation and conformational conversion of $G_3(T_2AG_3)_3$ released from the DNA duplex by BLM helicase monitored by gel electrophoresis. Unwinding in a 150 mM K^+ solution in the absence (a) or in the presence (b) of 40% (w/v) PEG 200 was initiated by the addition of ATP at 37 °C, and samples were examined by gel electrophoresis at the indicated time after unwinding initiation. K^+ and K^+/PEG indicate the $G_3(T_2AG_3)_3$ prepared in K^+ and K^+/PEG solution with heat denaturation/renaturation used as reference for antiparallel/parallel and parallel G-quadruplex, respectively. dsDNA is the DNA duplex before unwinding. The intramolecular nature of the G-quadruplexes was reflected by their fast migration compared with that of the 21 nt poly-T (T21).[6a]

the human telomere G-quadruplex has a sedimentation coefficient that is 24.9% smaller than that of the antiparallel/parallel hybrid form[17a] and, as a result, migrates slower in gel electrophoresis.[6a] In the K^+ solution, the $G_3(T_2AG_3)_3$ formed an antiparallel/parallel hybrid structure upon release from the duplex, as judged from the two reference structures, and it remained in this form over time (Figure 4 a). From Figure 4 b, it is apparent that in the K^+/PEG solution, the $G_3(T_2AG_3)_3$ initially also formed an antiparallel/parallel hybrid structure with a faster migration. This structure slowly transformed to the parallel one, which showed a slower migration. The slow conversion is in agreement with the CD data in Figure 1 and with previous results from our research group and others.[6a,19]

The parallel/antiparallel hybrid human telomere G-quadruplex features a (3 + 1) G-quartet core, in which three G-tracts are oriented in one direction and another in the opposite direction.[11b,c,13,20] This structure can have several variants according to the order of the loop arrangement, which is affected by cations, quadruplex-binding drugs, and flanking sequences.[2c,11b,c,13,20] To better resolve the structure identified in our experiments, we next analyzed the G-quadruplex by using a ligand-induced photocleavage footprinting technique that we developed recently.[21] This technique identifies the orientation of each of the four G-tracts in a G-quadruplex using the ligand tetrakis(2-trimethylaminoethylethanol) phthalocyaninato zinc tetraiodine (Zn-TTAPc), which induces differential cleavages to the guanines between the two terminal G-quartets under UV irradiation; therefore, the orientation of each G-tract can be revealed by comparing the relative extent of guanine cleavage at its two ends. In this analysis, the core sequence was flanked by TTA at both the 5′ and 3′ ends in order to efficiently precipitate the cleavage fragments and separate them on gel.[21] G-quadruplexes at the equilibrium state were prepared by heat denaturation/renaturation.[6a]

In Figure 5, it can be seen that the DNA released from the duplex in a K^+ solution adopted a ↓↑↓↓ orientation corresponding to the antiparallel/parallel (3 + 1) hybrid structure

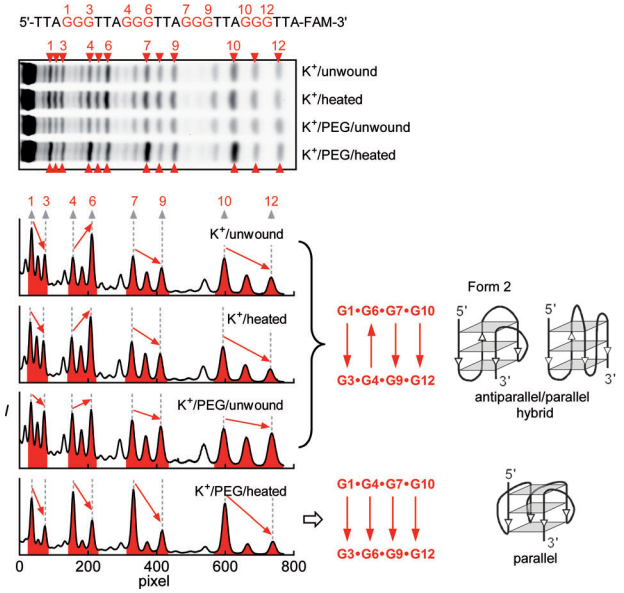

Figure 5. Zn-TTAPc induced photocleavage of $(T_2AG_3)_4T_2A$ released from the DNA duplex by BLM helicase in a 150 mM K^+ solution in the absence and presence of 40% (w/v) PEG 200. The image at the top shows the footprinting electrophoresis gel, and the graphs at the bottom indicate the densitometry profile of the corresponding gel lanes. The bands indicated by red arrowheads and the peaks in red correspond to guanines that participated in the G-quartet formation. The red arrows in the graph were drawn according to the intensity of the first and last peaks of each G-tract and then combined to obtain the folding orientations of the G-tracts. The ↓↑↓↓ orientation in the upper three graphs indicates two possible isoforms (schemes on the right) that differ in the second TTA loop (lateral and diagonal, respectively). The form 2 structure has been reported to be adopted by the sequence $(T_2AG_3)_4T_2A$[21] and $TAG_3(T_2AG_3)_3T_2$[20] in a K^+ solution. The ↓↓↓↓ orientation in the lower graph corresponds to a parallel G-quadruplex.[21]

with the first, third, and fourth G-tract in one direction and the second in the opposite direction, which is identical to the structure adopted in heat denaturation/renaturation. When released in the K^+/PEG solution, the DNA also adopted a ↓↑↓↓ orientation, as judged from the relative cleavage of the two guanines at the two ends of the four G-tracts, as well as from the general cleavage pattern. In contrast, the DNA subjected to heat denaturation/renaturation showed a ↓↓↓↓ orientation corresponding to the parallel G-quadruplex. These results indicate that the DNA, when liberated in both

the K^+ and K^+/PEG solution, folded into the same antiparallel/parallel (3 + 1) hybrid structure. The unwinding in a K^+/PEG solution could not reach 100% (see Figure S3 in the Supporting Information), so that a small fraction of the duplex was present, in which all the guanines were similarly cleaved.[21] This result may explain why the difference of cleavage between the two guanines at the ends of a G-tract was smaller than that observed in the absence of PEG. In comparison with previous results, the introduction of TTA at the two ends of the core sequence did not affect the folding conformation.

The four independent analyses provided convincing evidence that, when liberated from the duplex in a K^+/PEG solution, the human telomere sequences $G_3(T_2AG_3)_3$ and $T_2AG_3(T_2AG_3)_3T_2A$ initially adopt an antiparallel/parallel (3 + 1) hybrid G-quadruplex rather than the parallel one they adopt at the equilibrium state in the same solution. The fact, that the same structure was obtained with the different sequences in Figures 1 and 3–5 suggests that the presence of flanking sequences did not alter the antiparallel/parallel hybrid nature of the G-quadruplex. Since the structure adopted at the equilibrium state is the most stable one under the given conditions, the initial formation of the antiparallel/parallel hybrid G-quadruplex implies that the structure was favored by kinetics rather than stability. This behavior suggests that the formation kinetics played an important role in determining the initial conformation of the G-quadruplex. In a K^+ solution without PEG, the kinetic structure was the same as the thermodynamic structure.

Kinetic studies revealed that telomere DNA folds into a G-quadruplex within microseconds, which is often followed by additional isomerization on a time scale ranging from seconds to hundreds of seconds.[22] The later decrease in fluorescence in Figure 3a might suggest such an isomerization process. By fitting the three curves in Figure 3a to a sequential two-step first-order reaction model (see Figure S4 in the Supporting Information), a rate constant of 0.015 s^{-1} was obtained for this possible isomerization that corresponds to a relaxation time of 65 s. Since the duplex unwinding is 2–3 orders of magnitude slower than the folding of telomere DNA,[16,22c] the fluorescence traces in Figure 3a,b depict the time courses of unwinding and accumulation of G-quadruplexes. The fitting of Figure 3a provided a rate constant of 0.22 s^{-1} for the unwinding in a K^+ solution. For the unwinding in a K^+/PEG solution, the fitting of Figure 3b to a simple first-order model provided a smaller rate constant of 0.02 s^{-1}. The unwinding, the G-quadruplex folding, and the following isomerization are much faster than the extremely slow conversion of telomere DNA from the kinetic (3 + 1) hybrid to the thermodynamic structure (Figure 4b);[6a] this conversion has a rate constant of 9.56×10^{-5} s^{-1} or a relaxation time of 2.9 h.[19] This fact suggests that the initial G-quadruplex formation and isomerization that followed shortly are of more physiological significance than the much slower long-term conversion.

The human telomere sequence was used for this study because it is a simple and well-characterized model system for G-quadruplex folding; however, the strand release by BLM helicase is more relevant to situations where a complementary strand is present. For double-stranded telomere DNA, G-rich strand separation occurs when it is transcribed[23] or replicated. The single-stranded telomere overhang can be bound by proteins such as POT1.[24] The strand releasing may also approximate that upon dissociation of DNA binding proteins. Our observation raises the possibility that a G-quadruplex, when allowed to fold in vivo, may not adopt the structure that it adopts at the equilibrium state. This behavior adds more complexity to the physiological relevance of G-quadruplex structures formed by human telomere DNA and likely other nucleic acids in terms of molecular recognition and interaction. When a G-rich telomere DNA is liberated, its initially assumed structure determines how it will be first recognized in interactions with other molecules. A better understanding of the physiological relevance of G-quadruplex structures will require more information on the mechanism of G-quadruplex folding regulation, competition, and interconversion between structural variants.

In summary, we have studied the kinetic and thermodynamic control of the folding of G-quadruplexes and demonstrated how they may affect the selection of G-quadruplex conformation. The conformational distinction between the telomere DNA structures that were produced by the two folding pathways emphasizes the need to consider folding kinetics in addition to thermodynamic stability with respect to the biological and pharmaceutical relevance of G-quadruplex structures. In this regard, the large number of G-quadruplex structures identified so far at the equilibrium state may need to be re-evaluated.

Received: March 11, 2011
Revised: May 30, 2011
Published online: July 14, 2011

Keywords: DNA · folding topology · G-quadruplexes · kinetic control · thermodynamic control

[1] a) H. M. Wong, L. Payet, J. L. Huppert, *Curr. Opin. Mol. Ther.* **2009**, *11*, 146–155; b) T. M. Ou, Y. J. Lu, J. H. Tan, Z. S. Huang, K. Y. Wong, L. Q. Gu, *ChemMedChem* **2008**, *3*, 690–713; c) S. Neidle, *FEBS J.* **2010**, *277*, 1118–1125.

[2] a) D. H. Zhang, G. Y. Zhi, *J. Biotechnol.* **2010**, *150*, 6–10; b) D. H. Zhang, T. Fujimoto, S. Saxena, H. Q. Yu, D. Miyoshi, N. Sugimoto, *Biochemistry* **2010**, *49*, 4554–4563; c) T. I. Gaynutdinov, R. D. Neumann, I. G. Panyutin, *Nucleic Acids Res.* **2008**, *36*, 4079–4087; d) J. Dai, M. Carver, D. Yang, *Biochimie* **2008**, *90*, 1172–1183.

[3] a) P. Hazel, J. Huppert, S. Balasubramanian, S. Neidle, *J. Am. Chem. Soc.* **2004**, *126*, 16405–16415; b) A. Bugaut, S. Balasubramanian, *Biochemistry* **2008**, *47*, 689–697.

[4] a) I. N. Rujan, J. C. Meleney, P. H. Bolton, *Nucleic Acids Res.* **2005**, *33*, 2022–2031; b) N. Smargiasso, F. Rosu, W. Hsia, P. Colson, E. S. Baker, M. T. Bowers, E. De Pauw, V. Gabelica, *J. Am. Chem. Soc.* **2008**, *130*, 10208–10216.

[5] a) E. M. Rezler, J. Seenisamy, S. Bashyam, M. Y. Kim, E. White, W. D. Wilson, L. H. Hurley, *J. Am. Chem. Soc.* **2005**, *127*, 9439–9447; b) H. Zhang, X. Xiao, P. Wang, S. Pang, F. Qu, X. Ai, J. Zhang, *Spectrochim. Acta Part A* **2009**, *74*, 243–247; c) X. Wang, J. Huang, Y. Zhou, S. Yan, X. Weng, X. Wu, M. Deng, X. Zhou, *Angew. Chem.* **2010**, *122*, 5433–5437; *Angew. Chem. Int. Ed.* **2010**, *49*, 5305–5309.

[6] a) Y. Xue, Z. Y. Kan, Q. Wang, Y. Yao, J. Liu, Y. H. Hao, Z. Tan, *J. Am. Chem. Soc.* **2007**, *129*, 11185 – 11191; b) D. Miyoshi, A. Nakao, N. Sugimoto, *Biochemistry* **2002**, *41*, 15017 – 15024; c) D. Miyoshi, H. Karimata, N. Sugimoto, *Angew. Chem.* **2005**, *117*, 3806 – 3810; *Angew. Chem. Int. Ed.* **2005**, *44*, 3740 – 3744.

[7] D. Yang, K. Okamoto, *Future Med. Chem.* **2010**, *2*, 619 – 646.

[8] a) R. Hänsel, F. Löhr, S. Foldynová-Trantírková, E. Bamberg, L. Trantírek, V. Dötsch, *Nucleic Acids Res.*, DOI: 10.1093/nar/gkr174; b) D. Miyoshi, H. Karimata, N. Sugimoto, *J. Am. Chem. Soc.* **2006**, *128*, 7957 – 7963; c) V. Víglaský, K. Tluckova, L. Bauer, *Eur. Biophys. J.* **2011**, *40*, 29 – 37; d) T. Fujimoto, D. Miyoshi, H. Tateishi-Karimata, N. Sugimoto, *Nucleic Acids Symp. Ser.* **2009**, 237 – 238; e) J. Zhou, C. Wei, G. Jia, X. Wang, Q. Tang, Z. Feng, C. Li, *Biophys. Chem.* **2008**, *136*, 124 – 127.

[9] a) D. Miyoshi, K. Nakamura, H. Tateishi-Karimata, T. Ohmichi, N. Sugimoto, *J. Am. Chem. Soc.* **2009**, *131*, 3522 – 3531; b) Z. Y. Kan, Y. Lin, F. Wang, X. Y. Zhuang, Y. Zhao, D. W. Pang, Y. H. Hao, Z. Tan, *Nucleic Acids Res.* **2007**, *35*, 3646 – 3653; c) Z. Y. Kan, Y. Yao, P. Wang, X. H. Li, Y. H. Hao, Z. Tan, *Angew. Chem.* **2006**, *118*, 1659 – 1662; *Angew. Chem. Int. Ed.* **2006**, *45*, 1629 – 1632; d) K. W. Zheng, Z. Chen, Y. H. Hao, Z. Tan, *Nucleic Acids Res.* **2010**, *38*, 327 – 338.

[10] a) W. Li, D. Miyoshi, S. Nakano, N. Sugimoto, *Biochemistry* **2003**, *42*, 11736 – 11744; b) D. Miyoshi, S. Matsumura, S. Nakano, N. Sugimoto, *J. Am. Chem. Soc.* **2004**, *126*, 165 – 169.

[11] a) W. Li, P. Wu, T. Ohmichi, N. Sugimoto, *FEBS Lett.* **2002**, *526*, 77 – 81; b) A. Ambrus, D. Chen, J. Dai, T. Bialis, R. A. Jones, D. Yang, *Nucleic Acids Res.* **2006**, *34*, 2723 – 2735; c) Y. Xu, Y. Noguchi, H. Sugiyama, *Bioorg. Med. Chem.* **2006**, *14*, 5584 – 5591.

[12] a) C. C. Hardin, E. Henderson, T. Watson, J. K. Prosser, *Biochemistry* **1991**, *30*, 4460 – 4472; b) R. Jin, B. L. Gaffney, C. Wang, R. A. Jones, K. J. Breslauer, *Proc. Natl. Acad. Sci. USA* **1992**, *89*, 8832 – 8836; c) P. Balagurumoorthy, S. K. Brahmachari, D. Mohanty, M. Bansal, V. Sasisekharan, *Nucleic Acids Res.* **1992**, *20*, 4061 – 4067; d) L. Petraccone, E. Erra, L. Nasti, A. Galeone, A. Randazzo, L. Mayol, G. Barone, C. Giancola, *Int. J. Biol. Macromol.* **2003**, *31*, 131 – 137.

[13] K. N. Luu, A. T. Phan, V. Kuryavyi, L. Lacroix, D. J. Patel, *J. Am. Chem. Soc.* **2006**, *128*, 9963 – 9970.

[14] G. N. Parkinson, M. P. Lee, S. Neidle, *Nature* **2002**, *417*, 876 – 880.

[15] a) M. C. Miller, R. Buscaglia, J. B. Chaires, A. N. Lane, J. O. Trent, *J. Am. Chem. Soc.* **2010**, *132*, 17105 – 17107; b) M. M. Dailey, M. C. Miller, P. J. Bates, A. N. Lane, J. O. Trent, *Nucleic Acids Res.* **2010**, *38*, 4877 – 4888; c) V. Dapic, V. Abdomerovic, R. Marrington, J. Peberdy, A. Rodger, J. O. Trent, P. J. Bates, *Nucleic Acids Res.* **2003**, *31*, 2097 – 2107; d) S. Masiero, R. Trotta, S. Pieraccini, S. De Tito, R. Perone, A. Randazzo, G. P. Spada, *Org. Biomol. Chem.* **2010**, *8*, 2683 – 2692.

[16] J. Q. Liu, C. Y. Chen, Y. Xue, Y. H. Hao, Z. Tan, *J. Am. Chem. Soc.* **2010**, *132*, 10521 – 10527.

[17] a) J. Li, J. J. Correia, L. Wang, J. O. Trent, J. B. Chaires, *Nucleic Acids Res.* **2005**, *33*, 4649 – 4659; b) T. Kimura, K. Kawai, M. Fujitsuka, T. Majima, *Chem. Commun.* **2006**, 401 – 402; c) T. Kimura, K. Kawai, M. Fujitsuka, T. Majima, *Tetrahedron* **2007**, *63*, 3585 – 3590.

[18] S. M. Law, R. Eritja, M. F. Goodman, K. J. Breslauer, *Biochemistry* **1996**, *35*, 12329 – 12337.

[19] L. Xu, S. Feng, X. Zhou, *Chem. Commun.* **2011**, *47*, 3517 – 3519.

[20] A. T. Phan, K. N. Luu, D. J. Patel, *Nucleic Acids Res.* **2006**, *34*, 5715 – 5719.

[21] K. W. Zheng, D. Zhang, L. X. Zhang, Y. H. Hao, X. Zhou, Z. Tan, *J. Am. Chem. Soc.* **2011**, *133*, 1475 – 1483.

[22] a) R. D. Gray, L. Petraccone, J. O. Trent, J. B. Chaires, *Biochemistry* **2010**, *49*, 179 – 194; b) R. D. Gray, J. Li, J. B. Chaires, *J. Phys. Chem. B* **2009**, *113*, 2676 – 2683; c) R. D. Gray, J. B. Chaires, *Nucleic Acids Res.* **2008**, *36*, 4191 – 4203.

[23] C. M. Azzalin, P. Reichenbach, L. Khoriauli, E. Giulotto, J. Lingner, *Science* **2007**, *318*, 798 – 801.

[24] P. Baumann, T. R. Cech, *Science* **2001**, *292*, 1171 – 1175.

